Arch. Metall. Mater. **63** (2018), 2, 987-992

DOI: 10.24425/122432

K. MICHALEK*#, M. TKADLEČKOVÁ*, L. SOCHA*, K. GRYC*, M. SATERNUS**#,
J. PIEPRZYCA**, T. MERDER**

# PHYSICAL MODELLING OF DEGASSING PROCESS BY BLOWING OF INERT GAS

This paper deals with the possibilities of using physical modelling to study the degassing of metal melt during its treatment in the refining ladle. The method of inert gas blowing, so-called refining gas, presents the most common operational technology for the elimination of impurities from molten metal, e.g. for decreasing or removing the hydrogen content from liquid aluminium. This refining process presents the system of gas-liquid and its efficiency depends on the creation of fine bubbles with a high interphase surface, uniform distribution, long period of its effect in the melt, and mostly on the uniform arrangement of bubbles into the whole volume of the refining ladle. Physical modelling represents the basic method of modelling and it makes it possible to obtain information about the course of refining processes. On the basis of obtained results, it is possible to predict the behaviour of the real system during different changes in the process. The experimental part focuses on the evaluation of methodical laboratory experiments aimed at the proposal and testing of the developed methods of degassing during physical modelling. The results obtained on the basis of laboratory experiments realized on the specific physical model were discussed.

*Keywords:* physical modelling, refining ladle, inert gas blowing, degassing process, impeller

## 1. Introduction

Due to the increasing demand for aluminium casting quality, emphasis has increasingly been placed on the melt refining processes by removing gases (hydrogen) [1-4], metallic impurities (sodium, calcium, lithium, etc.) and non-metallic impurities (oxides, nitrides, borides, carbides, etc.) [5] during processing. The most common method for removing impurities is the method of inert gas blowing. This type of refining is the most widely used technology [6-13], with possibilities for optimization.

Under operating conditions, however, it is difficult to perform optimization of the refining technology; therefore, simulation methods are preferred as more beneficial. Modelling processes is a method that aims at capturing the behaviour of a real system using a physical or mathematical model [14-22] without having to interfere with a real technological process and thereby limit the standard production process. Based on the results obtained on the model, it is possible to predict the behaviour of the real system in the course of various process changes. Another added value of the active use of modelling methods is the possibility of visualizing processes that contribute to understanding the processes taking place in real systems (ladle) [23].

The essence of physical modelling consists in the targeted utilization of the similarities of the processes that take place within the actual device (work) and its model. Both the work and the model have the same physical nature in physical modelling. This means that fluid flow is modelled again by fluid flow, but at a certain scale of lengths, velocities of volume flow, viscosity, etc. The basic condition for transferring results from the model to the work is the similarity of the processes going on in the work and the model.

## 2. Experimental conditions of physical modelling

To model the process of degassing the aluminium melt by inert gas blowing, the physical modelling method is quite widely used, for example. Liquid aluminium is mostly simulated by water, which is mainly used for its availability, low cost, environmental friendliness, and especially due to the fact that the dynamic viscosity of water and liquid aluminium is very close [24,25]. A comparison of the basic parameters of aluminium and water is given in Table 1.

Laboratory experiments were conducted in accordance with the theory of similarity between the model and the work, based on the identity of Froude's criterion. In terms of the construction of the aggregate representing the refining ladle and the modelling conditions, it is necessary to observe in particular:

- geometrical similarity of the work and its model,
- dynamic similarity of fluid flow in the work and its model.

* VŠB-TECHNICAL UNIVERSITY OF OSTRAVA, FACULTY OF METALLURGY AND MATERIALS ENGINEERING, DEPARTMENT OF METALLURGY AND FOUNDRY AND REGIONAL MATERIALS SCIENCE AND TECHNOLOGY CENTRE, 17. LISTOPADU 15/2172, OSTRAVA-PORUBA, CZECH REPUBLIC
** SILESIAN UNIVERSITY OF TECHNOLOGY, FACULTY OF MATERIALS ENGINEERING AND METALLURGY, UL. KRASIŃSKIEGO 8, KATOWICE, POLAND
# Corresponding author: karel.michalek@vsb.cz; mariola.saternus@polsl.pl

TABLE 1

Comparison of basic physical parameters of the aluminium melt and water

| Parameter | Aluminium | Water |
|---|---|---|
| Temperature – $T$, K | 1023 | 293 |
| Density – $\rho$, kg·m$^{-3}$ | 2345 | 998.5 |
| Dynamic viscosity – $\mu$, Pa·s | 0.00120 | 0.00101 |
| Kinematic viscosity – $\nu$, m$^2$·s$^{-1}$ | $0.51 \cdot 10^{-6}$ | $1.012 \cdot 10^{-6}$ |
| Surface tension – $\sigma$, N·m$^{-1}$ | 0.680 | 0.072 |

Physical modelling was focused on the process of liquid aluminium degassing by inert gas (argon) blowing over a rotating graphite impeller. The experiments carried out were aimed at assessing the suitability of the proposed modelling methodology, as well as gaining the primary knowledge of the influence of two relevant refinement parameters on the hydrogen content behaviour during refining, namely:

- inert gas flow rate,
- rotary impeller speed.

The model can also be used to assess the impact of the baffles, the influence of the depth of immersion of the rotary impeller and the effect of various modifications of the rotary impeller endings.

Experiments investigating degassing the metal melt with inert gas were performed in the Laboratory of Physical and Numerical Modelling at the Department of Metallurgy and Foundry, FMMI (Faculty of Metallurgy and Materials Engineering), VŠB – TU Ostrava. In the laboratory, a physical refining ladle model was constructed on a 1:1 scale to a pilot plant warm refining ladle model, which at the same time corresponded to a 1:2.03 scale to an operational refining ladle with a capacity of 1800 kg of aluminium melt.

Fig. 1 shows a physical model assembly including baffles for inhibiting fluid rotation, and Fig. 2 shows a detail of the inert gas feed rotary impeller used. The presented rotary impeller is patented, therefore it is not possible to show detailed dimensions.

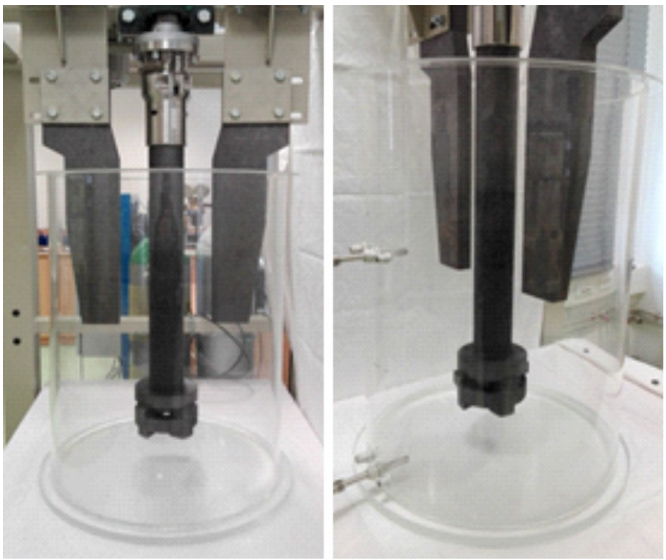

Fig. 1. Physical model assembly: refining ladle, rotary impeller, 2× baffles and measuring probe

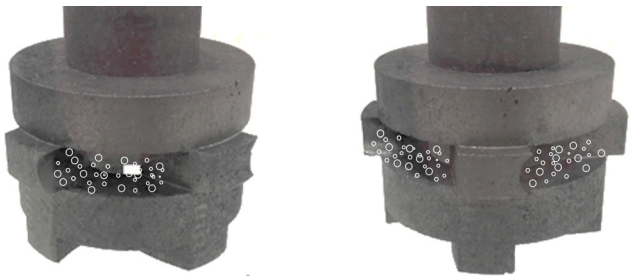

Fig. 2. Detail of the impeller head for physical modelling

The change of the impeller immersion was solved by a hydraulically controlled platform on which the actual ladle model made of Plexiglas was placed. Variable and controlled rotary impeller speeds were resolved using an asynchronous motor powered through an inverter. Mass flowmeters and needle valves were used to measure and regulate the flow of gases (argon and oxygen).

The decrease in hydrogen content in aluminium melt during inert gas refining was simulated on the physical model by a decrease in the dissolved oxygen content in the model liquid (water). Prior to each experiment, water was saturated with gaseous oxygen to the value of 23 ppm (23 mg $O_2 \cdot 1^{-1}$ of water). The actual experiment was then started at the moment when the inert gas (argon) was blown through the impeller with the simultaneous start of its rotation. For continuous measurement of the oxygen content, two optical fluorescence probes were used to measure the dissolved oxygen content up to 26 ppm, which were placed in two different positions of the ladle model. Fig. 3 shows basic dimensional data of physical model, including the location of the measuring probes.

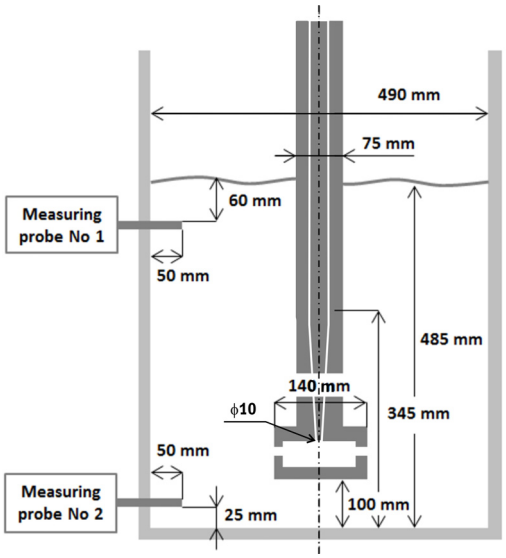


Fig. 3. Basic physical model dimension data

During rotating and blowing of inert gas there is an intense formation of gas-liquid mixture with very fine bubbles (0.005-0.015 m) which increase refining efficiency. Under normal operating conditions, baffles are commonly used to

prevent dangerous surface ripple and vortex formation. For this reason, two baffles were used on the physical model during the experiments, which are also used on a warm model in pilot-scale conditions.

### 3. Experiments performed and their evaluation

During the pilot modelling phase, experiments were conducted to assess the influence of rotary impeller speeds (350, 500 and 650 rpm) and flow rate of refining gas (5, 10 and 15 Nl·min$^{-1}$). Table 2 shows individual experimental variants (the presented data refer only to model conditions, no information about real conditions was included due to proprietary patent information).

TABLE 2

Characteristics of methodical variants of physical modelling

| Variant | Rotary impeller speeds; rpm | Flow rate of Ar; Nl · min$^{-1}$ |
|---|---|---|
| A | 350 | 5.0 |
| B | | 10.0 |
| C | | 15.0 |
| D | 500 | 5.0 |
| E | | 10.0 |
| F | | 15.0 |
| G | 650 | 5.0 |
| H | | 10.0 |
| I | | 15.0 |

The experiments were then evaluated and processed in the charts in Fig. 4. The charts characterize the course of oxygen concentration reduction during refining with argon. In addition, during the experiments, the photographs shown in Fig. 5 were taken; they documented the character of the liquid flow, and the behaviour and distribution of the generated blown argon bubbles for variants A through I.

While analysing the results presented in Fig. 4, it was found that the course of the change in oxygen concentration measured by both probes (Nos. 1 and 2) was almost identical. This trend is associated with high rate of turbulence, causing an apparently almost homogeneous concentration field in the entire volume of the refining tank. Thus, it can be stated that the decrease in oxygen concentration had the same character both in the lower and the upper part of the refining ladle.

In addition, a comparison of the chart set in Fig. 4 was carried out where the influence of the rotary impeller speed at different inert gas flows is graphically compared. From the recorded degassing process shown in Fig. 4 it is clear that for the given experimental conditions, the increase in rotary impeller speed has a more positive effect on the degassing process than the increase in the flow rate of the refining gas. From the results in Fig. 4, which are successively devoted to the variation in oxygen content at different speeds and argon flow rates in the range of 5 Nl·min$^{-1}$ to 15 Nl·min$^{-1}$, it follows that the rising rotary impeller speed of 350 rpm to 650 rpm significantly reduces the time to reduce the oxygen concentration to a value close to 0 ppm. It is also clear from the curves (Fig. 4a-c) that, with increasing rotary impeller speed, the effect of the increasing argon flow becomes less pronounced.

Subsequently, an assessment of the nature of the internal flow, behaviour and distribution of generated blown argon bubbles for the individual variants according to Fig. 5 was made.

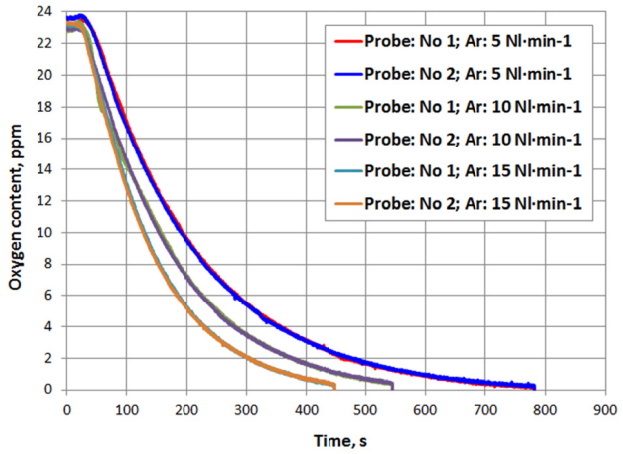


a) rotary impeller speed: 350 rpm

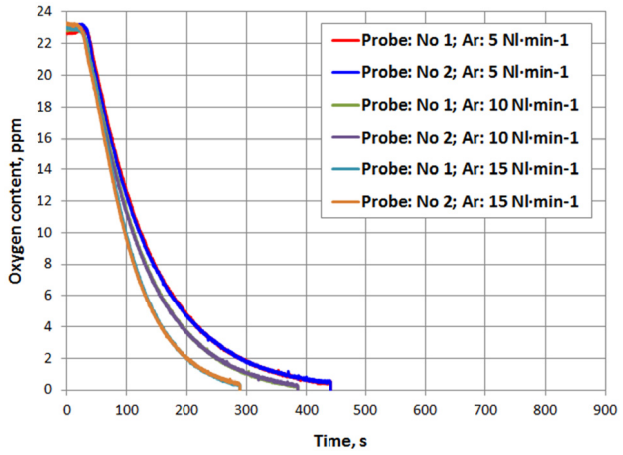


b) rotary impeller speed: 500 rpm

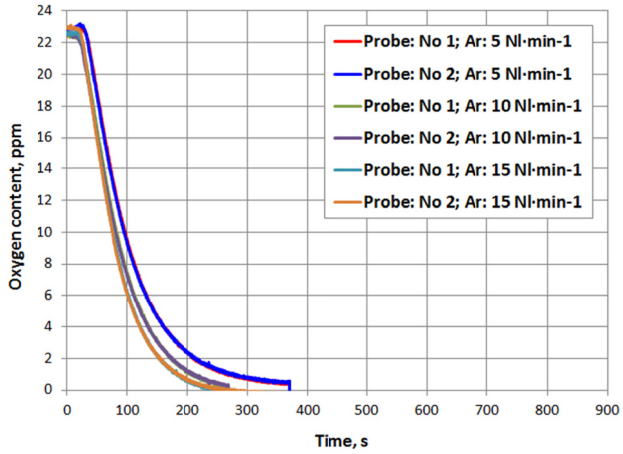


c) rotary impeller speed: 650 rpm

Fig. 4. Change in oxygen content at different rotary impeller speeds and Ar flows in the range of 5 Nl·min$^{-1}$ to 15 Nl·min$^{-1}$

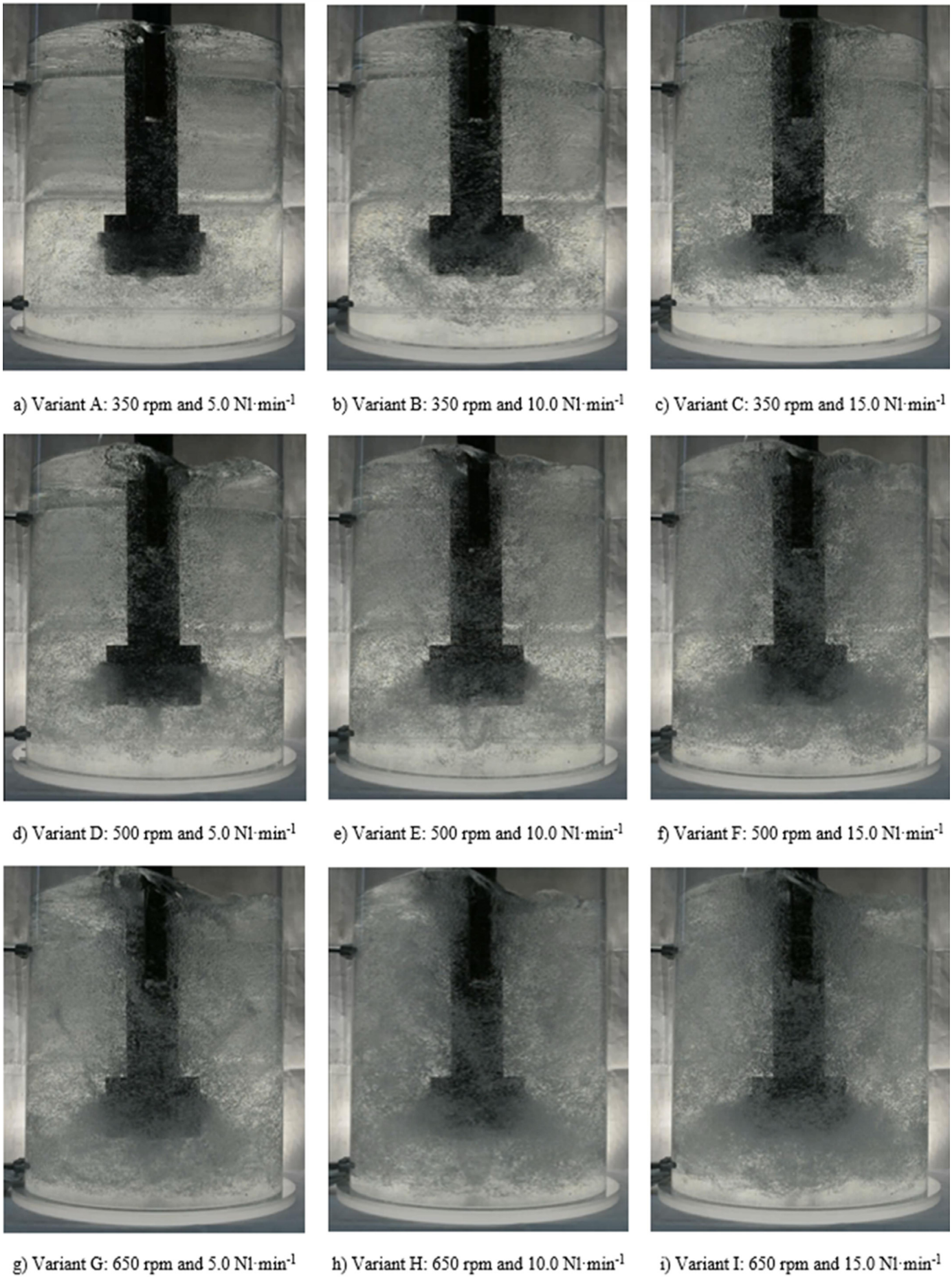

a) Variant A: 350 rpm and 5.0 Nl·min$^{-1}$ b) Variant B: 350 rpm and 10.0 Nl·min$^{-1}$ c) Variant C: 350 rpm and 15.0 Nl·min$^{-1}$

d) Variant D: 500 rpm and 5.0 Nl·min$^{-1}$ e) Variant E: 500 rpm and 10.0 Nl·min$^{-1}$ f) Variant F: 500 rpm and 15.0 Nl·min$^{-1}$

g) Variant G: 650 rpm and 5.0 Nl·min$^{-1}$ h) Variant H: 650 rpm and 10.0 Nl·min$^{-1}$ i) Variant I: 650 rpm and 15.0 Nl·min$^{-1}$

Fig. 5. Example of the internal flow character, behaviour and distribution of the generated blown Ar bubbles for variants A to I

The above-mentioned photographs show the effect of increasing rotary impeller speeds in the range of 350 rpm to 650 rpm, when bubbles are distributed more intensely to the entire volume of the refining ladle. The photographs also show the negative effect of rising rotary impeller speeds on intense surface ripple, even when using two baffles.

In addition to increasing speed, the effect of the increasing argon flow rate was also monitored in the range of 5 Nl·min$^{-1}$ to 15 Nl·min$^{-1}$. Also in this case it can be stated that the increasing flow is manifested by a significant increase in the number of bubbles produced in the entire volume of the refining ladle, which has a positive effect on the rate of reduction of the oxygen concentration representing the degassing.

Finally, Fig. 6 shows quantitative comparison of the order of each of the variants according to the time required to reduce the oxygen content in the water to a value close to 0 ppm. In this chart, the individual rotary impeller speeds are colour differentiated, with argon flows inside the columns. The variants were then sorted from the best (the shortest times) to the worst (the longest times). Not only from the bar chart in Fig. 6, but also from the previous charts in Fig. 4, it is obvious that for each colour-differentiated rotary impeller speed that is more important for the given impeller and baffles configuration, better times were achieved at higher gas flows. Fig. 6 also shows a nonlinear trend of increasing time to achieve low oxygen content with decreasing rotary impeller speed.

Compared to the previous discussion, however, it is apparent in Fig. 6 that in some cases, namely Variant F and C, better results are achieved at lower rotary impeller speeds and higher gas flow than at higher rotary impeller speeds and lower inert gas flows (Variants G and D). This fact is significant when considering the negative effect of higher rotary impeller speed on the surface ripple, which is unfavourable in view of the possibility of re-oxidation and bringing dirt into the melt volume from its surface. The effect of the rotary impeller speed and the flow of argon on the surface stability (ripple) and bubble character is illustrated in more detail by the series of photographs in Fig. 5.

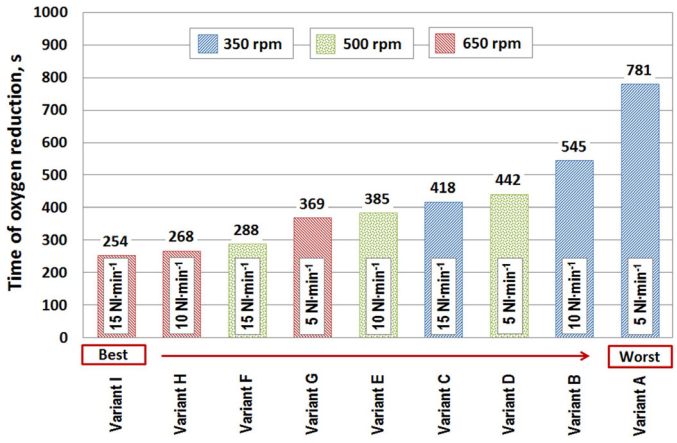


Fig. 6. Quantitative evaluation of the efficiency of each variant according to the time of oxygen content reduction in the water to a value close to 0 ppm

## 4. Conclusion

Under laboratory conditions, methodological and pilot experiments were conducted to test the methodology of physical modelling of degassing of the aluminium melt.

The results were evaluated on the basis of changes in the oxygen content dissolved in water during the inert gas blowing through the rotating impeller.

From the results of the physical modelling, it can be stated that the optical fluorescence probes used allow a correct measurement of the course of the oxygen content reduction in the water. On the basis of a series of experiments, a measurement methodology was developed, including a way of evaluating the results. In addition, a procedure for imaging experiments under suitable conditions was created representing video series and photographs. At the same time, a significant influence of the rotary impeller speed and flow rate of refining gas on the process of the oxygen content reduction in the water was demonstrated.

Further experimental work will focus on the assessment of other relevant degassing conditions, as well as on the transfer of the achieved results to the operating conditions.

**Acknowledgements**

The work was created under the support of the Czech Ministry of Industry and Trade within the frame of the programme TRIO in the solution of the projects reg. No. FV10080 “Research and Development of Advanced Refining Technologies of Aluminium Melts for Increase in Product Quality” and project No. LO1203 “Regional Materials Science and Technology Centre - Feasibility Program” funded by the Ministry of Education, Youth and Sports of the Czech Republic and from the support of “Student Grant Competition” projects, No. SP2018/77 and SP2018/60.

This paper was created with the financial support of Polish Ministry for Science and Higher Education under internal grant BK-221/RM0/2018 for Faculty of Materials Engineering and Metallurgy, Silesian University of Technology, Poland.

## REFERENCES

[1] S. Kato, Sumitomo Light Metal Technical Report **34**, 59-77 (1993).
[2] P.N. Anyalebechi, Light Metals Conference, TMS,857-872 (2003).
[3] M. Saternus, J. Botor, Metalurgija **48**, 175-179 (2009).
[4] L. Zhang, X. Lv, A. Tryg Torgerson, M. Long, Mineral processing&Extractive Metall. Rev. **32**, 150-228 (2011).
[5] C.J. Simensen, G. Berg, ALUMINIUM **56**, 335-340 (1980).
[6] M. Hernández-Hernández, J.L. Camacho-Martinéz, C. Gonzáles--Rivera, M.A. Ramiréz-Argáez. Journal of Materials Processing Technology **236**, 1-8 (2016).
[7] M.B. Taylor, M.C.G. Belanger, E.D. Adams, Light Metals, TMS 779-784 (2000).
[8] G. Mealand, E. Myrbostad, K. Vegas, Light Metals, TMS 855-859 (2002).

[9] J.M. Chateau, Aluminium Times **04/05**, 34-35 (2003).
[10] P. Le Brun, Light Metals, TMS 869-875, (2002).
[11] K.A. Carpenter, M.J. Hanagan, Light Metals, TMS 1017-1020 (2001).
[12] Y. Liu, T. Zhang, M. Sano, Q. Wang, X. Ren, J. He,Trans. of Nonferrous Metals Society of China **21**, 1896-1904, (2011).
[13] J.W. Evans, A. Field, N. Mittal, Light Metals, TMS 909-913, (2003).
[14] E. Waz, J. Carre, P. Le Brun, A. Jardy, C. Xuereb, D. Ablitzer, Light Metals, TMS 901-907 (2003).
[15] J.L. Song, F. Chiti, W. Bujalski, A.W. Nienow, M.R. Jolly, Light Metals, TMS 743-748 (2004).
[16] E.R. Gomez, R. Zenit, C.G. Rivera, G. Trapaga, A. Ramirez-Argaez, Metallurgical and Materials Transaction B **44B**, 974-983 (2013).
[17] J.L. Camacho-Martinez, M.A. Ramizrez-Argaez, A. Juarez-Hernandez, C. Gonzalez-Rivera, G. Trapaga-Martinez, Materials and Manufacturing Proces **27,** 556-560 (2012).
[18] F. Kerdouss, P. Proulx, J.F. Bilodeau, S. Vaudreuil, Light Metals, TMS 793-795 (2004).
[19] A. Fjeld, S. Edussuriya, J.W. Evans, A. Mukhopadhyay, Light Metals, TMS 963-968 (2005).
[20] B. Panic, J. Janiszewski, Metalurgija, **53**, 331-334 (2014).
[21] M. Warzecha, Metalurgija **50**, 147-150 (2011).
[22] T. Merder, J. Pieprzyca, M. Saternus, Metalurgija **53**, 155-158 (2014).
[23] K. Michalek, Využití fyzikálního a numerického modelování pro optimalizaci metalurgických procesů, VŠB Ostrava, **2001**, ISBN 80-7078-861-5 (in Czech).
[24] M. Saternus, J. Botor, Archives of Metallurgy and Materials **55**, 463-475 (2010).
[25] M. Saternus, Metalurgija **50**, 257-260 (2011).